We are IntechOpen, the world's leading publisher of Open Access books Built by scientists, for scientists

4,800
Open access books available

122,000
International authors and editors

135M
Downloads

Our authors are among the

154
Countries delivered to

TOP 1%
most cited scientists

12.2%
Contributors from top 500 universities

CLARIVATE ANALYTICS BOOK CITATION INDEX INDEXED

WEB OF SCIENCE™

Selection of our books indexed in the Book Citation Index in Web of Science™ Core Collection (BKCI)

Interested in publishing with us?
Contact book.department@intechopen.com

Numbers displayed above are based on latest data collected.
For more information visit www.intechopen.com

18

Digital Filtering Techniques to Reduce Image Noise and Improve Dose Resolution in X-Ray CT Based Normoxic Gel Dosimetry

N. Gopishankar[1], S. Vivekanandhan[1], A. Jirasek[2], S. S. Kale[1], G. K. Rath[1]
Sanjay Thulkar[1], V. Subramani[1], S. Senthil Kumaran[1] and R. K. Bisht[1]
[1]*All India Institute of Medical Sciences, New Delhi,*
[2]*Department of Physics and Astronomy, University of Victoria, B.C.*
[1]*India*
[2]*Canada*

1. Introduction

Gel dosimetry is a promising technique for the implementation of 3D dose verification within the radiation therapy clinic, since it is the only methodology which provides comprehensive 3D dose measurement of conformal treatments such as Intensity Modulated Radiation Therapy (IMRT), Stereotactic radiosurgery (SRS) and Stereotactic Radiotherapy (SRT), and volumetric arc therapies (VMAT). In polymer gel dosimetry, monomer molecules polymerize and are fixed in the gel matrix when exposed to radiation. The spatial dose information thus can be obtained by gel imaging. Gel imaging methods which are currently under investigation are MRI, optical computed tomography and x-ray computed tomography. While promising, x-ray CT images of irradiated polymer gel exhibit low contrast due to small change in density that occurs during polymerization. The response of CT contrast to dose is weak and noise reduction is critical in order to achieve adequate dose resolution in gel dosimetry using x-ray computed tomography. Ideally, image noise is minimized using high tube current, long scan times and high number of image averages [Hilts et al 2005]. Digital image filtering is an effective method in reducing image noise while maintaining accurate spatial dose information. Generally it is performed in either frequency domain or spatial domain. In a previous work, several spatial filters were applied to Stereotactic Radiosurgery (SRS) irradiated polymer gel image [Hilts and Duzenli 2004]. In their study it was found that the two highest performing filters were the adaptive mean (Wiener) and smallest univalue segment assimilating nucleus (SUSAN). In another study a new method of signal to noise ratio (SNR) enhancement by 2D two-point maximum entropy regularization method (TPMEM) was investigated [Jirasek 2006]. However, a comprehensive examination of the best performing filters from these two studies has not been undertaken. Here, we test the Weiner and TPMEM digital filters on X-ray CT image of the irradiated PAGAT gel in order to reduce noise and improve dose resolution. This work builds off of previous studies and evaluates and compares the highest-performing filters from past individual works [Hilts and Duzenli 2004, Jirasek et al 2006].

1.1 Concept of dose resolution

Dose resolution or minimal detectable difference (MDD) in dose is one of the most important features of gel dosimeter [Baldock et.al. PMB 2001]. In general, $D^p\Delta$ is related to σ_D which is the standard deviation or dose uncertainty in the measured dose.

$$D^p\Delta = K_P\sqrt{2}\,\sigma_D \quad (1)$$

Where Kp is the coverage factor for coincidence interval p. σ_D is the standard deviation of the sample. Dose resolution ($D^{95\%}\Delta$) is defined as the minimal separation between two absorbed doses such that they may be distinguished with a given level of confidence, p. For a 95% confidence level the dose resolution becomes $D^{95\%}\Delta = 2.77.\sigma_D$.

In CT gel dosimetry, σ_D is due to uncertainty in measured N_{CT} (σN_{CT}) and in the dose response curve for a linear dose response, σ_D is related to σN_{CT} by the slope of the response.

$$\sigma_D = [\partial D/\partial N_{CT}]\,\sigma N_{CT} \quad (2)$$

Combining Equation (1) an (2), $D^p\Delta$ is improved by a decrease in the slope of the dose to N_{CT} response and as investigated here a decrease in σN_{CT}.

1.1.1 Theory

1.1.1.1 CT image noise

Noise in CT images is primarily due to quantum noise inherent in photon detection and electronic noise. Quantum noise results from counting a finite number of random events (photons hitting the detector) and is, theoretically, Poisson distributed. A characteristic of Poisson distributions is that the variance equals the mean. That is for Poisson distributed noise the variance depends on signal strength (number of photons counted). In theory, noise in CT projection data should display this characteristic. However the noise in a final CT image is Gaussian distributed due to the presence of electronic noise. As a result, the noise characteristics of a CT imaged depend on the scan parameters and reconstruction algorithm used [Hilts 2004].

1.1.1.2 Digital image filtering

The gel images used to evaluate filters in this project has been preprocessed for artifact removal using image averaging and background subtraction [Hilts and Jirasek 2008] and its image degradation is predominantly caused by noise. Mask-based filters are all based on a similar principle: a mask (m x n pixels) is centered on each pixel of the image, g(s,t), and a function is applied to the image pixels in the region of the mask (Sxy) so that the center pixel is replaced with a new value, f(x,y). The TPMEM filter is not based on a masking approach but, rather, the minimization of an entropy and fidelity function, as described below.

For this study slope of linear region (0 to 12 Gy) from calibration gel was used to calculate σ_D. The filters are applied to a gel irradiated CT image of a simulated clinical treatment. For all cases, the effects of filter kernel size, number of filter iterations, and TPMEM stopping criterion are investigated.

1.2 Filters used for noise reduction in this study

1.2.1 Adaptive filter

Adaptive filters are a class of filters for which filtering power is adapted based on local image statistics. The adaptive mean or Wiener filter is a spatial filter based on moving kernel (similar to a traditional mean filter). The difference lies in that the adaptive filter weights its filtering power based on the ratio of the local variance (σ^2_L) to the overall image noise (σ^2_N). The filtered value is given by

$$f(x,y) = g(x,y) - ((\sigma^2_L) / (\sigma^2_N))*[\, g(x,y) - m_L \,] \quad (3)$$

where g(x,y) is the unfiltered value and m_L is the local mean value of the image. All image filtering was performed in Matlab (The Mathworks, Natick, MA, USA), which provides a built-in function for this adaptive mean filter.

1.2.2 TPMEM

The aim of TPMEM is to minimize the function

$$T = -S + \lambda \chi^2 \quad (4)$$

where S is the entropy function, χ^2 is the chi square statistic which characterizes the degree of agreement between the initial (unsmoothed) and recovered (smoothed) full dataset and λ is a Lagrange multiplier that is to be determined. The balance between recovered data smoothness and fidelity is optimized by Lagrange multiplier λ.

Recently, the traditional TPMEM algorithm has been extended to (i) incorporate an additional parameter (X, see equation 5) to allow for a user defined tuning of the ratio between smoothness and image fidelity, and (ii) allow for the minimization to occur in 2D, as opposed to 1D spectra, as was originally reported. [Jirasek 2006 and Foist 2010].

$$T = -S + X \lambda \chi^2 \quad (5)$$

The underlying theory of TPMEM is presented in detail elsewhere (Greek et al 1995, Jirasek et al 2006).

2. Materials and methods

2.1 Gel preparation

Normoxic gel was prepared under normal atmospheric conditions. The components used for the preparation of the dosimeter were 6% gelatin (300 Bloom from Porcine skin), 3% Acrylamide, 3% N, N' methylene-bis-acrylamide (BIS), 88% distilled water and 10mM tetrakis(hydroxy methyl) phosphonium chloride (THP). (All from Sigma Aldrich, India). For preparation of PAGAT gel, 6% of gelatin by total weight of the dosimeter was mixed with 88% distilled water and allowed to soak for 45 minutes before heating to 50^{o}C in specially designed water bath with temperature control (thermostat), also crossed checked with a thermometer. A waterbath was designed in-house specifically to prepare 10 to 15 Liters of gel. The container with gelatin was heated to 50^{o}C and simultaneously stirred with overhead stirrer. BIS (3%) was added and stirred thoroughly in the gel solution till it

dissolved completely for 30 minutes. 3% Acrylamide was added subsequently and the whole content was stirred for an hour. Once a clear solution was obtained 10mM of THPC was added and stirred and the container was removed from water bath. A final volume of 4.5 Litres of gel was prepared. The gel was immediately poured into the three PET containers (each with 1mm thickness and 1500mL capacity) till screw top and tightly sealed with clingfilm and container lid. One container was used for calibration, one for clinical beam exposure and one for background subtraction purpose. The gel containers were immediately covered with black plastic cover to avoid exposure to daylight that might cause photopolymerization and then were refrigerated at 5^{o}C.

2.2 Gel calibration and irradiation

Irradiations were done approximately 23h post manufacture on a Varian Clinac2300CD linear accelerator (Varian Assoc., Palo Alto, CA). The PET containers (10cm diameter, 19cm height) for exposure were left in the linac room for 1 hr prior to irradiation. The first PET container (1) was irradiated to doses from 0 Gy to 14 Gy at D_{max} by large flask geometry method (Taylor et al. 2007). The second PET container (2) was irradiated with four intersecting 4 x 4cm^2 6MV field doses of 2, 5, 7, and 11Gy at the depth of maximum dose. The third PET container (3) was used for background subtraction. The background subtraction technique in general is successful in removing beam hardening artifacts and ring artifacts due to miscaliberated detector in the scanner. Reference marks were made on the containers for scanning reproducibility. After irradiation the gel containers were exposed to atmosphere one day after irradiation in order to make gels inactive and thus prevent further polymerization. Acquisition parameters for dose response experiments were as follows: tube voltage 140 kV, tube current 200 mA, scan time 1sec, FOV 130 x 130, image thickness 2.5 mm, Reconstruction algorithm B30 medium.

The relationship of N_{CT} to dose was obtained from the image of the calibration gel as shown in Figure 1. The average N_{CT} was measured for each region of uniform dose using MATLAB and a dose response curve was made. This curve was then used to convert the clinical treatment gel image into a dose map for quantitative image analysis. N_{CT} is shown as the value above background increases with dose. The response is well modeled by a linear function up to a dose of 12Gy, ($R^2 = 0.996$) with a slope of 222 cGy/H. Measured noise σN_{CT} (H) from region of interest in the gel exposed with clinical beams and calculated values of σ_D and dose resolution ($D^{95\%}\Delta$) were analyzed for dose regions in gel irradiated for simulated clinical treatment. The response had dose region of slope 222 cGy/H ($R^2 = 0.996$) and $D^{95\%}\Delta$ of 512.06 cGy.

2.3 Image filtering

The processed gel images were filtered using a Wiener filter described in Sec. 1.2.1 for 3x3, 5x5, 7x7, 11x11 pixel mask. All filtering was performed using MATLAB (Mathworks, USA). We further did filtering analysis with the TPMEM filter and compared those results with Wiener filter results. For this study we took several quantitative measures such as (i) profiles through the image (ii) FFT analysis of unfiltered image, Wiener filtered image and TPMEM filtered image (iii) SNR of filtered images (iv) root mean squared error (RMSE) (v) Pearsons correlation coefficient (PEARS). In order to compare RMSE with PEARS all the values quoted in this study are 1 – PEARS and are labeled as PEARSC.

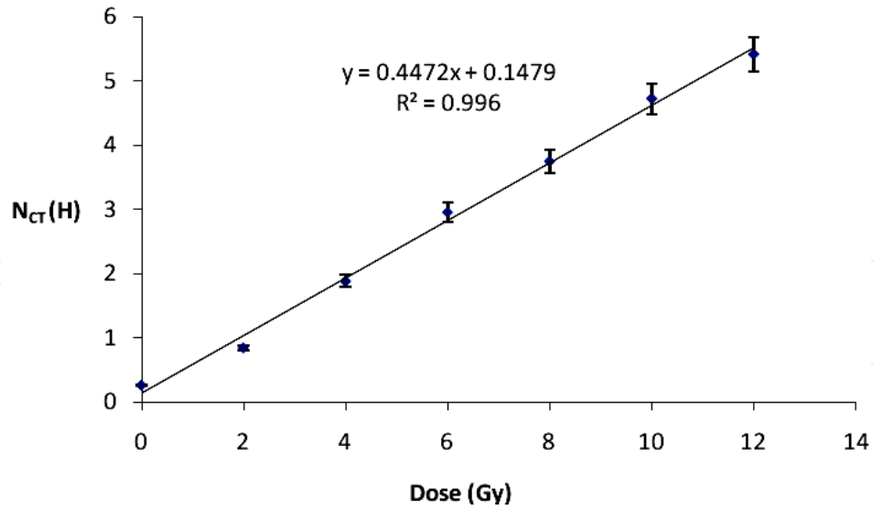

Fig. 1. Dose to N_{CT} response curve obtained from the calibration gel.

3. Results and discussions

3.1 Wiener filter

Figure 2 shows the radiation exposed gel image. The results of filtering the gel image with the filters described in Sec. 1.2.1 are shown in Table 1. In our study excellent dose resolution was obtained by applying adaptive mean filter with 11 x 11 pixel mask at second iteration which showed a $D^{95\%}\Delta$ of 24.65 cGy.

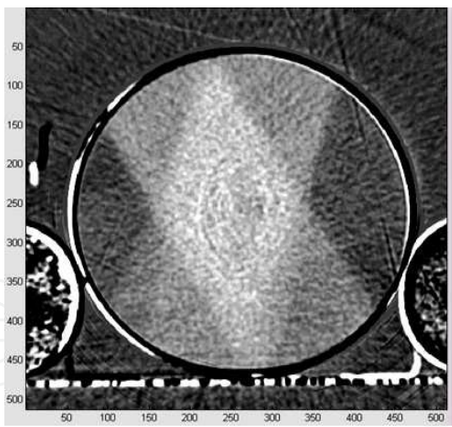

Fig. 2. X-ray CT image of gel in PET container irradiated with four intersecting 4 x 4cm^2 6MV field doses of 2, 5, 7, and 11Gy at the depth of maximum dose. This image was obtained after background subtraction and image averaging.

Measured σN_{CT} and calculated values of σ_D and $D^{95\%}\Delta$ are provided in Table 1 for Wiener filtered image and the unfiltered image. Results show that the improvement increases with the mask size as expected since a large mask provides a greater smoothing area.

Figure 3a represents the unfiltered gel image. Figure 3b and 3c represent the gel image after applying an 11 x 11 Wiener filter at first and second iteration respectively.

Filter	Mask	$\sigma N_{CT}(H)$	σ_D(cGy)	$D^{95\%}\Delta$ (cGy)	Profile Width
Unfiltered		0.8327	184.86	512.06	35.6174
Wiener filter	3 x 3	0.6270	139.19	385.56	34.3367
	5 x 5	0.5069	112.53	311.71	34.447
	7 x 7	0.3936	87.38	242.04	34.40312
	11 x 11(1st iteration)	0.1457	32.35	89.61	34.7228
	11 x 11(2nd iteration)	0.0401	8.90	24.65	33.881

Table 1. Summary of measured noise (σN_{CT}) and calculated dose uncertainty (σ_D) and dose resolution with 95% confidence ($D^{95\%}\Delta$) for the unfiltered and filtered images.

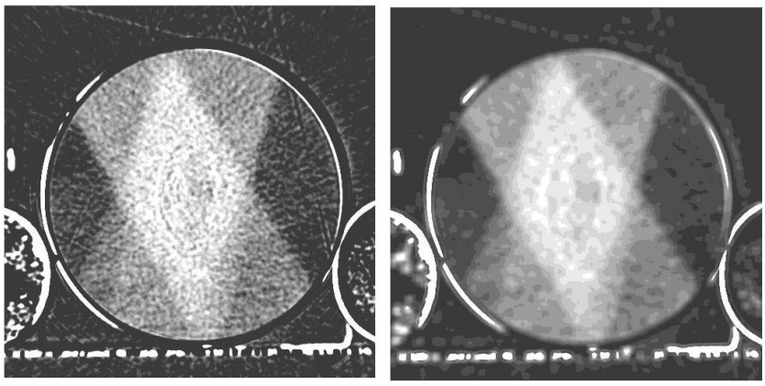

(a) (b)

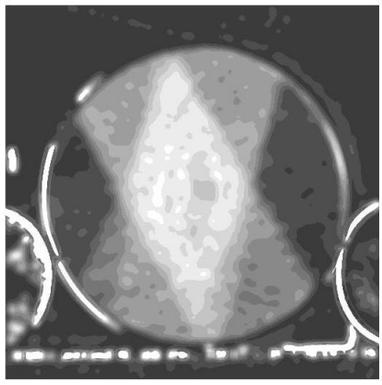

(c)

Fig. 3. (a) Unfiltered Image, (b) Wiener filtered Image (11 x 11 mask, 1st iteration), (c) Wiener filtered Image (11x11mask, 2nd iteration).

Figure 4a and 4b are horizontal and vertical profiles of the unfiltered and Wiener filtered images. The unfiltered gel image is characterized by several spikes throughout the profile. By applying Wiener filter the spikes are significantly reduced and smooth profile is obtained.

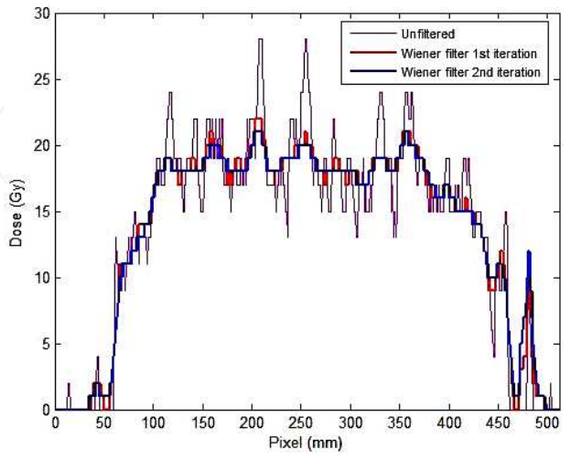

(a)

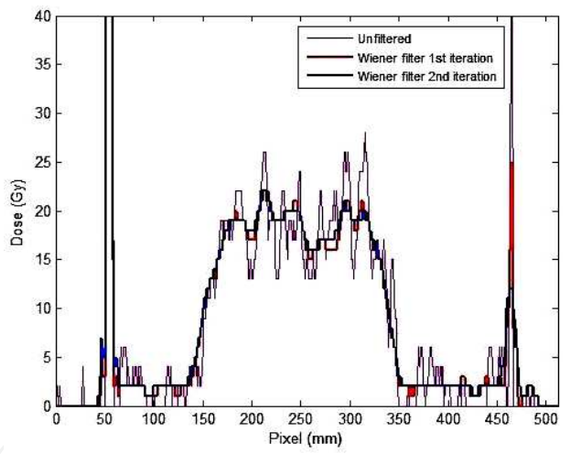

(b)

Fig. 4. (a) Horizontal Dose profiles for unfiltered image and Wiener filtered image 1st and 2nd iteration using 11 x 11 mask. (b) Vertical Dose profiles for unfiltered image and Wiener filtered image 1st and 2nd iteration using 11 x 11 mask.

In general, a tradeoff exists when increasing mask size. A larger mask generally improves image SNR, and hence dose resolution, but simultaneously degrades spatial dose information. In order to illustrate a typical spatial resolution degradation observed when applying a Wiener filter with 11x11 mask, we measured the width of the profiles in figure 4a (i.e. no iterations, 1, and 2 iterations of the Wiener filter). Table 1 illustrates that spatial degradation increases when applying the Wiener filters. Hence, a balance must be struck between image filtering and potential spatial degradation.

In Table 2 Wiener filter applied with different mask is shown. In Table 1 it was shown that as the mask size is increased the dose resolution is improved significantly. However the results of Table 2 showed different results. As the mask size increased the SNR value decreased. The SNR analysis of the unfiltered image showed SNR =1.272, and after Wiener filtering with 11x11 mask, SNR = 39.6049. RMSE and PEARSC values increased as the mask size was increased. By theory higher RMSE and PEARSC indicate poor filtering. The results prove that high filtering technique provides smoothness as shown in figure 3.c but at the same time causes image distortion.

Wiener Mask	RMSE	PEARSC	SNR
3 x 3	0.078	0.0019	2.3274
5 x 5	0.0927	0.0039	4.1234
7 x 7	0.1102	0.0057	7.1857
9 x 9	0.1285	0.0067	10.9466
11 x 11	0.1437	0.0088	19.7918
15 x 15	0.1634	0.018	39.6049
Unfiltered			1.272

Table 2. RMSE, PEARSC and SNR between unfiltered and Wiener filtering. Initial noisy data at SNR = 1.272.

3.2 TPMEM filter

In figure 5 TPMEM filter analysis is shown for the image matrix of size 96 x 96 pixels^2, i.e. the white-space around the gel container was cropped in order to decrease computation time. The actual matrix size of the unfiltered CT image used for noise reduction study was 512 x 512 pixels^2. For the a typical calculation time for a matrix of size 300 x 300 pixels^2 is approximately 20 minutes whereas for matrix of size 90 x 90 pixels^2 is around 40 seconds, hence we rescaled the CT image to a matrix of size 96 x 96 pixels^2. Figure 5 a, b, c and d are the unfiltered and TPMEM filtered CT image of the exposed gel for stopping criterion X = 0.5, 1.4 and 2.5 respectively. Increase in image smoothness can be seen as the stopping criterion is increased.

TPMEM Stopping Criterion	RMSE	PEARSC	SNR
X = 0.2	0.0371	0.001	1.4357
X = 0.5	0.0588	0.004	1.6685
X = 1.4	0.101	0.0145	2.2200
X = 1.6	0.1066	0.0173	2.3511
X = 1.8	0.1171	0.0217	2.4079
X = 2.0	0.1204	0.0239	2.6034
X = 2.5	0.1314	0.0353	3.5329
X = 4	0.1363	0.0394	4.0898
Unfiltered			1.2720

Table 3. RMSE, PEARSC and SNR between unfiltered and TPMEM filtering. Initial noisy data at SNR =1.272.

Other than SNR values, RMSE and PEARSC values for different stopping criterion were analyzed and the results are shown in Table 2. In the previous study it was shown that a

truly filtered image will contain high SNR, high PEARS (low PEARSC) and low RMSE [Jirasek et al 2006]. Hence, a tradeoff is again noted between image smoothness and fidelity.

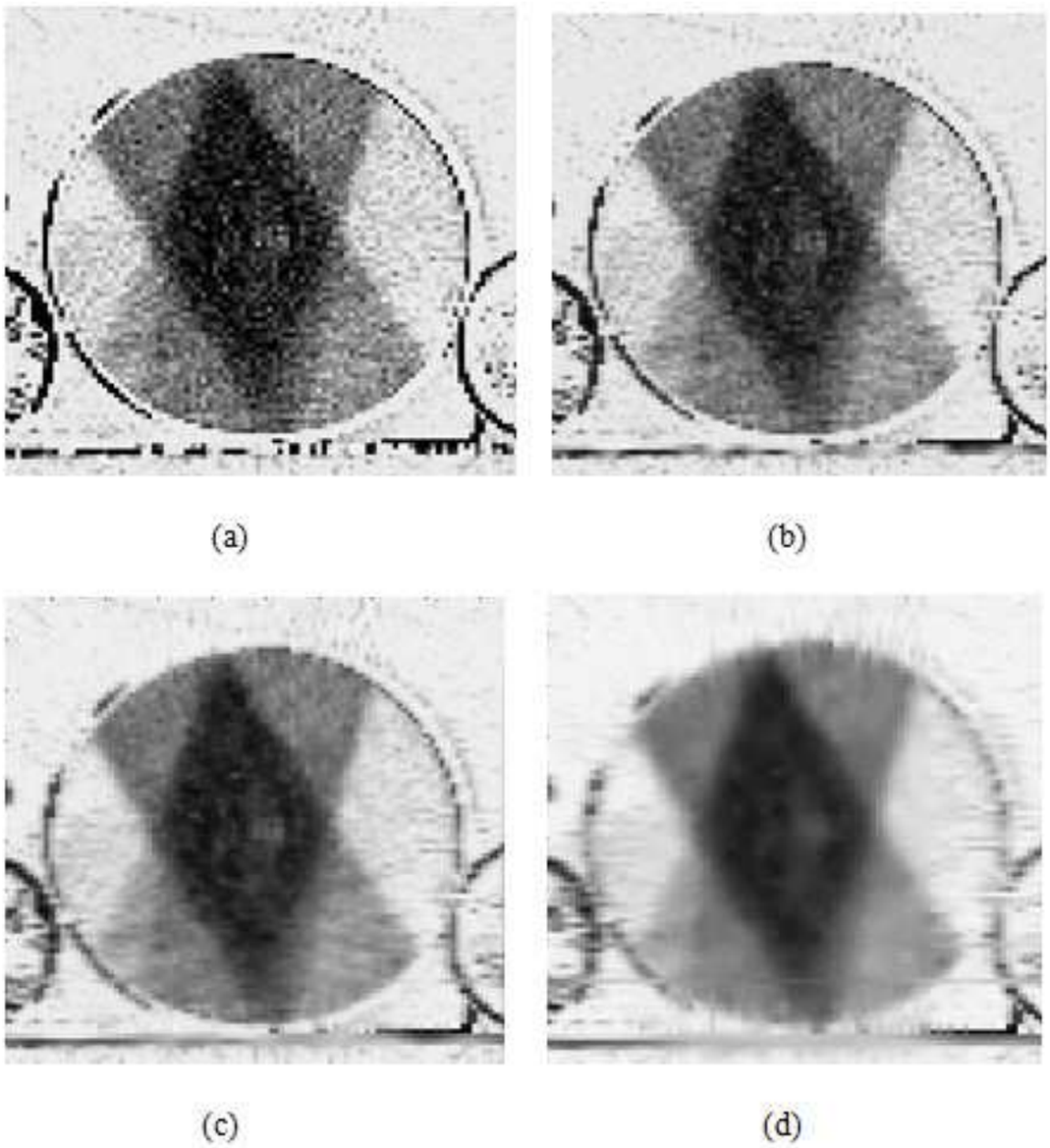

Fig. 5. TPMEM analysis for PAGAT gel image. (a) Unfiltered image. (b) TPMEM filtered image for stopping criterion X = 0.5. (c) TPMEM filtered image for stopping criterion X = 1.4. (d). TPMEM filtered image for stopping criterion X = 2.5.

Table 3 shows the actual SNR for the unfiltered image was SNR = 1.272 and after filtering with TPMEM with stopping criterion X = 0.5, 1.4, 2.5, SNR was observed to be 1.6685, 2.2200, 3.5329 respectively. However as the stopping criterion is increased further spatial degradation is observed as shown in figure 6.

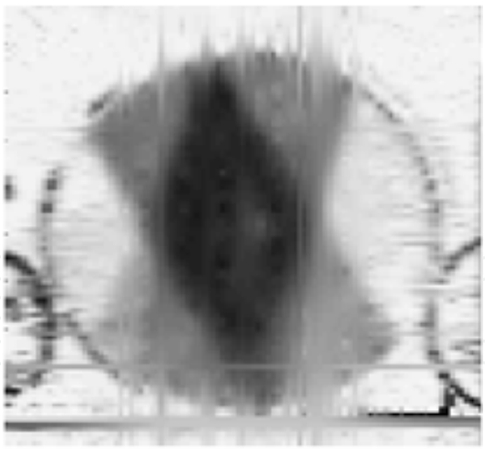

Fig. 6. Spatial degradation of image after filtering with TPMEM stopping criterion X = 4.

3.3 Filter comparison

Figure 7 (a) illustrates profiles taken through unfiltered and TPMEM filtered and Wiener filtered image. The profile comparison was done in the gel image which was rescaled to 96 x 96 pixels^2. The profiles show that Wiener filtered image profile is over smoothened were as the TPMEM filtered image still follows the peak and valley of the unfiltered image.

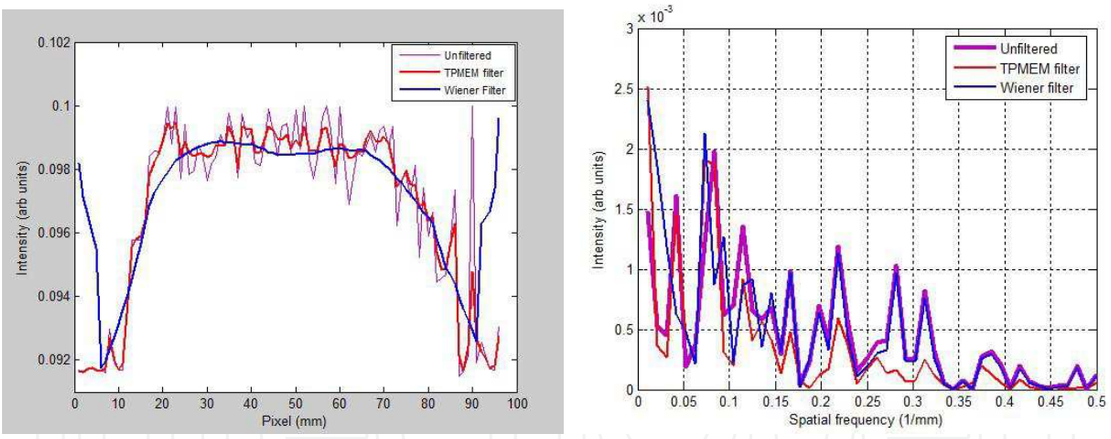

Fig. 7. (a) Profiles extracted through unfiltered, TPMEM filtered and Wiener filtered (11x 11 mask) image. (b) FFT data of the unfiltered and TPMEM filtered and Wiener filtered (11x 11 mask) image are shown in figures

In a previous study the TPMEM was applied to a SRS irradiated gel image [Jirasek et al 2006] which contains high dose gradients whereas in this work filtering was performed on four intersecting 4 x 4 cm^2 6MV fields with lower dose gradients as compared with the SRS study. Fast Fourier transform (FFT) data of the images are shown in figure 7 (b). TPMEM filtering is efficient in removing high frequency noise (> 0.15 mm^{-1}). It was also observed that TPMEM also retains much of the original signal in lower frequency regions (< 0.1 mm^{-1}). FFT results of Wiener filtered did not show any significant alterations in the FFT spectrum of the gel image.

4. Conclusion

In our study we found that dose resolution in CT images can be improved by applying spatial filters for removing noise. Adaptive Mean (Wiener) provided excellent dose resolution. Increasing kernel size and/or the number of filter iterations has a positive effect on noise reduction in filtered images. At the same time increasing kernel size and number of filter iterations become counterproductive, as image distortion (blurring) becomes unacceptably high. A recently developed filtering technique named TPMEM was also tested on the gel image. The TPMEM filter provided good SNR enhancement. Results indicate that CT imaging appears an attractive possibility for polymer gel dosimetry with such techniques available for improving SNR. In general the low filtering technique does not adequately smooth the images. In contrast, the high filtering technique provides smoothness but at the expense of some distortion of the shape. In particular, sharp contour changes are reduced by high filtering. Hence selection of appropriate filter and related parameters which control the fidelity and smoothness of filtered images is required before implementing it for X-ray CT polymer gel dosimetry. At present the TPMEM filters are useful for analysis of images with pixel size less than 300 x 300 pixels whereas the Adaptive mean filter can be applied to images of any size. Both the filters are capable of reducing image noise and improving dose resolution. In future application of filters to 3D image data will be of more importance.

5. Acknowledgements

We wish to gratefully acknowledge the support of AERB, India for this work through research project no N-964.

6. References

Baldock, C., Lepage. M., Back, S A J., Murry, P J., Jayasekara, P M., Porter, D. and Kron, T. (2001) Dose resolution in radiotherapy polymer gel dosimetry: effect of echo spacing MRI pulse sequence. Phys. Med. Biol, 46, 449.

Jirasek, A.,Mathews, Q.,Hilts, M.,Schulze, G., Blades, M. and Turner,R.(2006) Investigation of a 2D two-point maximum entropy regularization method for signal-to-noise ratio enhancement: application to CT polymer dosimetry. Phys. Med. Biol, 51, 2599-2617.

M. Hilts and A.Jirasek. Adaptive mean filtering for noise reduction in CT polymer gel dosimetry. Med. Phys. 35 (1), January 2008.

Hilts, M. and Duzenli, C.(2004) Image noise in x-ray CT polymer gel dosimetry. J Phys Conference Series, 3 252-256.

Hilts, M., Jirasek, A. and Duzenli, C. (2005) Technical considerations for implementation of x-ray CT polymer gel dosimetry, Phy Med Biol, 50, 1727 -1745.

Michelle Hilts., Cheryl Duzenli (2003) Image filtering for improved dose resolution in CT polymer gel dosimetry. Med. Phys. 31 (1), January 2004.

Jirasek. A., Hilts, M., Shaw, C. and Baxter, P. (2006) Investigation of tetrakis hydroxymethyl phosphonium chloride as an antioxidant for use in x-ray computed tomography polyacrylamide gel dosimetry. Physics in Medicine Biology, 51, 1891.

Taylor M L, Franich R D, Johnston P N, Millar R M and Trapp J V. (2007) Systematic variations in polymer gel dosimeter calibration due to container influence and deviations from water equivalence. Phys. Med. Bio, 52, 3991-4005.

R. B. Foist, H. G. Schulze, A. Jirasek, A. Ivanov, and R. F. B. T. Turner. A Matrix-Based Two-Dimensional Regularization Algorithm for Signal-to-Noise Ratio Enhancement of Multidimensional Spec- tral Data. Applied Spectroscopy, 64(11):1209–1219, Oct. 2010.

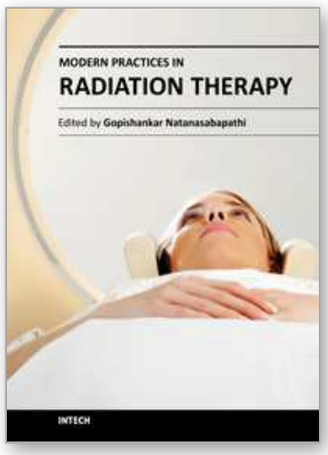

Modern Practices in Radiation Therapy

Edited by Dr. Gopishankar Natanasabapathi

ISBN 978-953-51-0427-8
Hard cover, 370 pages
Publisher InTech
Published online 30, March, 2012
Published in print edition March, 2012

Cancer is the leading cause of death in economically developed countries and the second leading cause of death in developing countries. It is an enormous global health encumbrance, growing at an alarming pace. Global statistics show that in 2030 alone, about 21.4 million new cancer cases and 13.2 million cancer deaths are expected to occur, simply due to the growth, aging of the population, adoption of new lifestyles and behaviors. Amongst the several modes of treatment for cancer available, Radiation treatment has a major impact due to technological advancement in recent times. This book discusses the pros and cons of this treatment modality. This book "Modern Practices in Radiation Therapy" has collaged topics contributed by top notch professionals and researchers all around the world.

How to reference

In order to correctly reference this scholarly work, feel free to copy and paste the following:

N. Gopishankar, S. Vivekanandhan, A. Jirasek, S. S. Kale, G. K. Rath Sanjay Thulkar, V. Subramani, S. Senthil Kumaran and R. K. Bisht (2012). Digital Filtering Techniques to Reduce Image Noise and Improve Dose Resolution in X-Ray CT Based Normoxic Gel Dosimetry, Modern Practices in Radiation Therapy, Dr. Gopishankar Natanasabapathi (Ed.), ISBN: 978-953-51-0427-8, InTech, Available from: http://www.intechopen.com/books/modern-practices-in-radiation-therapy/digital-filtering-techniques-to-reduce-image-noise-and-improve-dose-resolution-in-x-ray-ct-based-nor

INTECH
open science | open minds

InTech Europe
University Campus STeP Ri
Slavka Krautzeka 83/A
51000 Rijeka, Croatia
Phone: +385 (51) 770 447
Fax: +385 (51) 686 166
www.intechopen.com

InTech China
Unit 405, Office Block, Hotel Equatorial Shanghai
No.65, Yan An Road (West), Shanghai, 200040, China
中国上海市延安西路65号上海国际贵都大饭店办公楼405单元
Phone: +86-21-62489820
Fax: +86-21-62489821

IntechOpen